

MULTI-SCENARIO PREDICTION AND REGULATION STRATEGY OF CARBON BUDGET IN THE YELLOW RIVER BASIN OF CHINA UNDER THE “DOUBLE CARBON” TARGET

SHEN, W.^{1,2} – RONG, P. J.^{2,3*} – CAO, W. W.^{1*}

¹*College of Land and Tourism, Luoyang Normal University, Luoyang 471022 Henan, China
(e-mail: shenwei@henu.edu.cn)*

²*College of Geography and Environmental Science, Henan University / Key Laboratory of Geospatial Technology for the Middle and Lower Yellow River Regions, Henan University, Kaifeng 475004, China*

³*Urban and Rural Coordinated Development Center, College of Tourism and Exhibition, Henan University of Economics and Law, Zhengzhou, Henan, China*

**Corresponding authors
e-mail: rongpeijun@126.com; cwwjy5032@163.com*

(Received 25th Nov 2023; accepted 3rd May 2024)

Abstract. Under the increasingly severe climate crisis, it is of great significance to carry out research on carbon budget calculation and multi-scenario prediction under the “double carbon” target for realizing regional low-carbon and high-quality development. Taking the Yellow River Basin (YRB) of China as the research area, this paper firstly calculates the carbon budget of the YRB from 2000 to 2020 and analyzes its spatiotemporal change. Then, we simulated carbon emissions, carbon sequestration, and net carbon budget during 2030-2100 under the SSP1-5 scenario. Finally, the regulation strategies of carbon balance of the YRB were proposed from four aspects: strengthening ecological governance, improving land use mode, optimizing industrial structure and advocating low-carbon life. Our results showed: (1) The overall carbon sequestration and carbon emission show a trend of fluctuating increase during 2000 to 2020, but the increase rate of carbon emission is far greater than carbon storage. The net carbon emission during 2000-2020 is negative, which is manifested as a carbon sink area. (2) The order of carbon sequestration of the provinces in the YRB during 2030-2100 is the same under the SSP1-5 scenario, and the descending order is the following: Inner Mongolia, Qinghai, Shaanxi, Gansu, Shanxi, Henan, Ningxia, and Shandong. (3) The STIRPAT model can be used to predict the carbon emissions of the YRB in the future with high precision. (4) In terms of net carbon emissions, under the SSP1-5 scenario, the YRB will be a carbon sink area from 2030 to 2080, and a carbon source area from 2080 to 2100. (5) Different provinces have different paths to low-carbon development, Inner Mongolia and Qinghai maintain a good low-carbon development path under SSP1, SSP2 and SSP4 scenarios, Ningxia and Shandong maintain a good low-carbon development path under SSP1 and SSP2 scenarios, Shanxi maintains a good low-carbon development path under SSP1 and SSP3 scenarios, and Gansu, Shaanxi and Henan maintain a good low-carbon development path under the SSP3 scenario.

Keywords: *low-carbon development, carbon peaking, carbon neutrality, land use simulation, STIRPAT model, regulation strategy*

Introduction

Global warming has brought great threats to the environmental system on which human beings depend and resulted in a series of environmental risks such as melting glaciers, rising sea levels, extreme weather, and lack of resources (Mudryk et al., 2021; Regnier et al., 2022; Shen et al., 2023). The mitigation of climate change and the reduction of greenhouse gas emissions have become an urgent task for the sustainable development of human society. Since the implementation of the reform and opening

policy emphasizing economic development, energy-intensive industries of China have developed rapidly, and China became the world's largest emitter of carbon dioxide. Faced with the pressure of high growth in energy consumption, at the 2015 Paris Climate Conference, China committed to enhance the ratio of non-fossil energy in general energy consumption by 20% by 2030, so that the total carbon emissions will peak, and reach carbon neutrality by 2060 (Liu et al., 2015; Fang et al., 2019). Therefore, how to curb the growth of carbon emissions while maintaining economic development is a tremendous challenge for China. Carbon budget accounting is one of the important research topics in addressing global climate change, and it is also the basic path for countries and regions to build low-carbon cities and achieve emission reduction and foreign exchange increase (Wang and Li, 2020; Zhou et al., 2021). To come true the aim of carbon peaking and carbon neutrality, on the one hand, carbon emission reduction potential should be stimulated; on the other hand, carbon absorption efficiency should be improved to achieve a balance between emissions and absorption (Wang and Huang, 2019; Ji and Peta, 2021). Therefore, it is of great significance to carry out research on carbon budget accounting and future multi-scenario simulation for promoting low-carbon urban development and sustainable urban spatial planning.

For a long time, scholars have carried out a wealth of theoretical study and applied study on urban carbon emissions and carbon absorption. In terms of carbon emissions, existing studies mainly focus on the accounting methods of carbon emissions (measured method, model method, life cycle method, input-output method and IPCC carbon emission coefficient method) (Regnier et al., 2022; Han et al., 2022), space-time evolution (Jiang and Liu, 2021), driving mechanism (Mo and Wang, 2021), carbon reduction policy recommendations (Peng et al., 2023), and simulation prediction (STIRPAT model, BP neural network model, LEAP model) (Wang et al., 2020; Ma et al., 2020). Among them, the development of carbon emission accounting methods, space-time evolution rules, driving factors and other aspects has been relatively mature, while carbon emission simulation and prediction methods are still in the stage of continuous development and improvement. In terms of carbon absorption, as early as the 1960s, scholars began to explore carbon absorption accounting methods, mainly including vorticity correlation method, model simulation method, and sample site inventory method (Zhang et al., 2020; Tang et al., 2020). In the 21st century, with the evolution and application of 3S technology, a mass of scholars began to combine remote sensing image technology with the carbon sequestration capacity of ecological land and studied the spatial distribution of carbon uptake at different spatial scales by using remote sensing data of land use (Zhang et al., 2021; Zheng and Zheng, 2023). In terms of carbon sequestration prediction, existing studies mostly use land use prediction data simulated based on Markov-CA model, FLUS model, and PLUS model for spatial prediction of carbon sequestration (Wang et al., 2023; Xu et al., 2023). Through literature review and induction, it is found that the research content of carbon emission and carbon absorption is increasingly rich, and the research perspective is constantly expanding, which lays a foundation for the research of regional carbon budget balance and enriches the research context. However, there are still two shortcomings in the existing studies: First, few studies carry out multi-scenario simulation of carbon emission and carbon absorption at the same time and calculate the net carbon emission. Second, few studies have focused on long-term carbon budget series simulation based on SSP1-5 scenarios. Based on this, there is an urgent need to establish a multi-scenario integrated modeling framework that

integrates carbon emissions and carbon uptake to achieve the Sustainable Development Goals and support regional sustainable development.

The YRB is one of the most intensively populated and economically active regions in the world. Since the reform and opening up, with the rapid evolution of industry and the fleetly expansion of land urbanization, significant changes in regional ecological environment, economic scale, population scale and industrial structure have had a profound impact on the spatio-temporal distribution of carbon sources and sinks in the YRB. Hence, it is essential to calculate the carbon budget of the YRB and carry out multi-scenario forecast in the future. Based on this, this paper takes the YRB as the research area to carry out the multi-scenario prediction and regulation strategy of carbon budget in the YRB. The research process is shown in *Figure 1*: (1) The first part is a systematic accounting of carbon emission, carbon sequestration, and net carbon emissions during 2000 to 2020 on account of multi-source data. (2) The second part is a systematic analysis of land use distribution pattern in the YRB during 2030-2100 under the SSP1-5 scenario, and then a multi-scenario simulation of carbon sequestration stock in the Yellow River Basin during 2030-2100 is carried out by using a carbon uptake simulation model. (3) The third part is a multi-scenario simulation of carbon sequestration and carbon emission in the YRB during 2030-2100 using STIRPAT model. (4) The fourth part is to calculate the net carbon emissions during 2030-2100 under the SSP1-5 scenario based on carbon sequestration and carbon emission, and the temporal evolution of carbon balance in the YRB during 2030-2100 was analyzed. (5) Finally, we propose the regulation strategy of carbon balance from four aspects: strengthening ecological governance, improving land use mode, optimizing industrial structure and advocating low-carbon life.

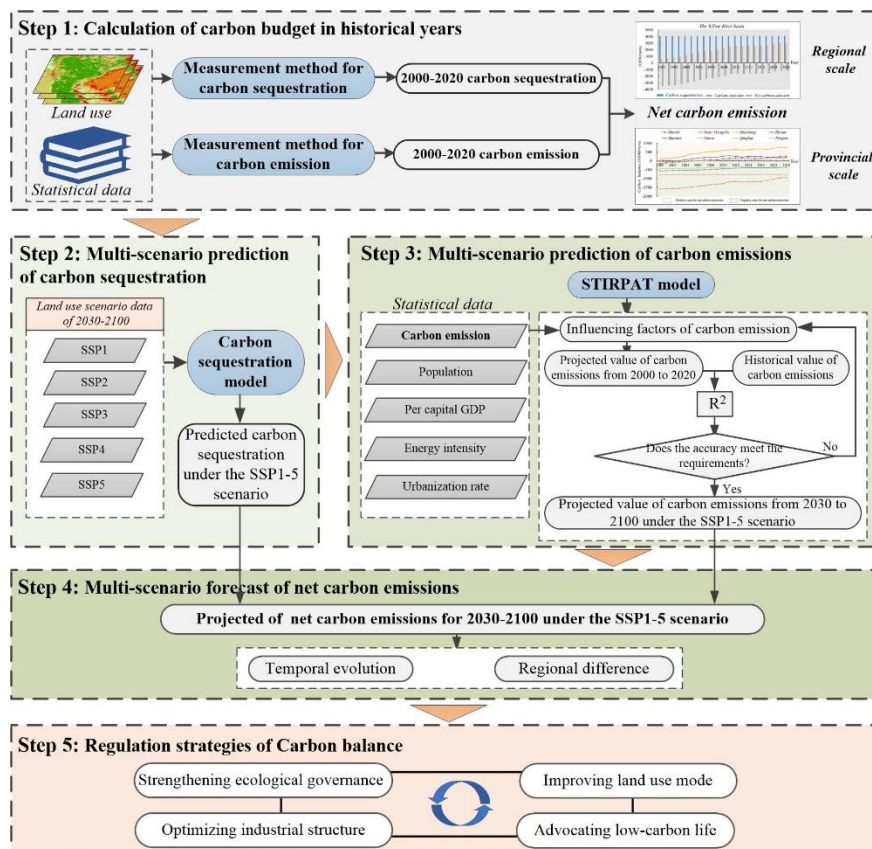


Figure 1. Framework of this study

Materials and methods

Research area

This study takes the Yellow River Basin (YRB) of China as the research area. The study region covers 8 provinces and regions flowing through the trunk stream of the Yellow River, incorporating 8 provincial administrative units: Shandong, Shanxi, Henan, Shaanxi, Ningxia, Inner Mongolia, Gansu, and Qinghai. The gross area of the research region is 2.55 million km² (Fig. 2), which spans the three major topographical steps of East and west. Influenced by the alternations of winter and summer monsoon and the surrounding terrain, the climate types are diverse, and the spatio-temporal distribution of precipitation is very uneven. As an important agricultural and urban agglomeration area in China, the YRB is one of the best densely populated regions in the world, and human social and economic activities are extremely intensive. Since reform and opening up, the speedy growth of population, the development of industry, and the speedy expansion of urbanization have caused profound changes in regional land use pattern, ecological landscape, water and soil environment, and carbon budget.

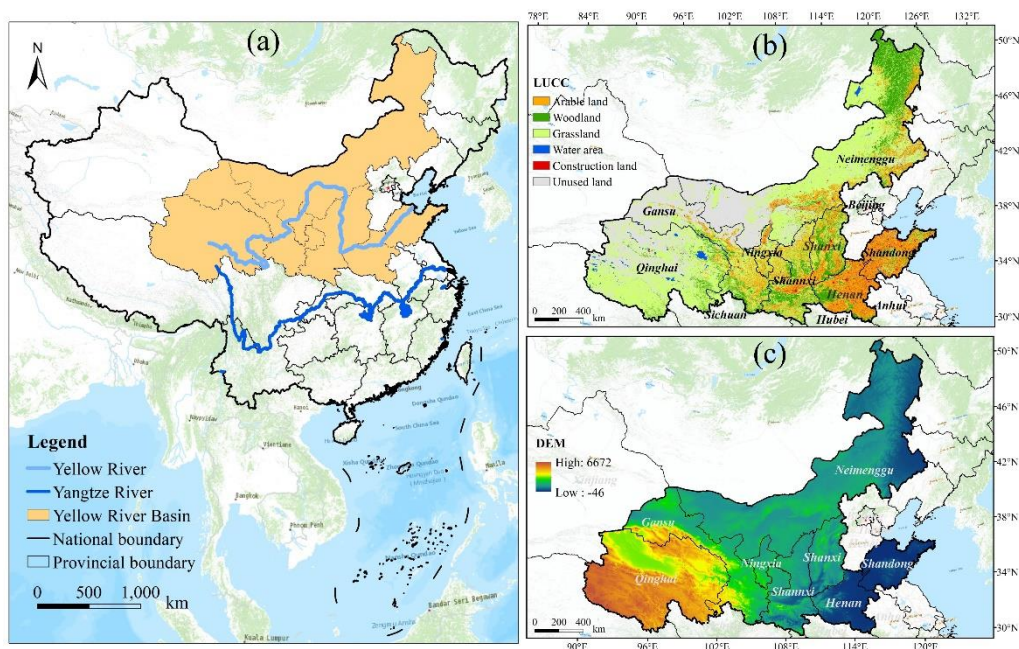


Figure 2. General overview map of the YRB: (a) The location map in China, (b) landuse map in 2020, and (c) elevation map

Data sources

Land use data for historical years (2000-2020) was obtained from the European Space Agency Climate Change Initiative (Bontemps et al., 2012). The multi-scenario landuse simulation data for the shared socioeconomic path (SSP) scenario considering socio-economic development status came from the research results of Luo et al. (2022), including SSP1 scenario, SSP2 scenario, SSP3 scenario, SSP4 scenario, and SSP5 scenario. The temporal resolution of the dataset is 2030-2100, and the spatial resolution is 1 km. The land use types of the dataset are spanided into 8 types (1-8 are construction land, farmland, grassland, shrub, forest land, water, bare land, desert, glacier, and snow).

Statistic data on population, per capita GDP, energy intensity, and urbanization level for eight provinces of Inner Mongolia, Qinghai, Shaanxi, Gansu, Shanxi, Henan, Ningxia, and Shandong from 2000 to 2020 are derived from the China Statistical Yearbook. The forecast data of provincial population and urbanization rate under different scenarios of SSP are originated from the study results of Chen et al. (2020). The forecast data of provincial GDP under the SSP1-5 scenario were derived from the study results of Wang et al. (2020), with a time series of 2030-2100 and a spatial resolution of 1 km (<https://zenodo.org/record/5768288#.YqFXccj5CWt>). The calculation process of energy intensity data in future years should refer to the research results of Huang et al. (2016).

Carbon emission calculation method

This study considers only the direct carbon emissions from fossil energy sources in the IPCC scope and divides the emission sources of urban energy activities into agriculture, industry, construction, transportation, services, other industries, and residential life. The formula is:

$$TCE = \sum_{t=1}^s CE_t \quad (\text{Eq.1})$$

$$CE_t = \sum_{i=1, j=1}^{mn} (E_{ij} \times F_j \times K_j) \quad (\text{Eq.2})$$

where TCE represents the total carbon emissions of energy consumption (unit is 10,000 tons). CE_t represents the carbon emissions in the t province, $t=1, 2, 3, \dots, 9$. E_{ij} is the total consumption of the i industry and the j energy, F_j is the coefficient of conversion of the j energy into standard coal, K_j is the carbon emission coefficient (Wang et al., 2019; Mo et al., 2021). $n=1, 2, 3, \dots, 7$; $m=1, 2, 3, \dots, 8$. The values of carbon emission coefficient and discount coal coefficient are shown in *Table 1*.

Table 1. Discount coal coefficient and carbon emission coefficient of various energy sources

Energy type	Discount coal coefficient (t standard coal /t)	Carbon emission coefficient (tons of carbon/tons of standard coal)
Raw coal	0.7143	1.9003
Coke	0.9714	2.8604
Crude oil	1.4286	3.0202
Gasoline	1.4714	2.9251
Kerosene	1.4714	3.0179
Diesel	1.4571	3.0959
Fuel oil	1.4286	3.1705
Natural gas	1.4286	2.1622

Calculation method of carbon sequestration

Different human utilization of land resources resulted in regional carbon emissions and carbon uptake, in which carbon emissions mainly came from energy consumption and human respiration, while carbon uptake was provided by the carbon sequestration function of terrestrial vegetation (Xia et al., 2019; Wang et al., 2021). Water area, unused land, farmland, forest, shrub, and grassland play the role of atmospheric carbon sink.

Cultivated land, woodland, shrub, grassland, water, and wetland as ecological land can achieve carbon absorption; Unused land such as bare land and glacier snow can also achieve carbon absorption (Xia et al., 2019; Wang et al., 2021). The calculation formula of carbon sequestration is:

$$CS_q = G_q \cdot S_q \quad (\text{Eq.3})$$

$$CS_{Total} = \sum_{q=1}^n CS_q \quad (\text{Eq.4})$$

where CS_q is the carbon absorption amount of the q species, and CS_{Total} is the carbon sequestration amount of all species. G_q is the carbon absorption coefficient of the q species (kg/m^2), and the carbon absorption coefficients of farmland, forest, shrub, grassland, bare land, water, glacier, and snow are 0.0007, 0.0657, 0.0161, 0.0138, 0.0005, 0.024 and 0.0005 (Xia et al., 2019; Wang et al., 2021, 2023). S_q stands for the land use area (m^2).

Carbon emission prediction method based on STIRPAT model

(1) Analysis of influencing factors

First, STIRPAT model was adopted to analyze the effects of population, per capita GDP, energy intensity, and urbanization rate on carbon emission (Jiao and Chen, 2012; Huang et al., 2016). The formula of STIRPAT model is as follows:

$$\ln I = \ln a + \beta_1 \ln P + \beta_2 \ln A + \beta_3 \ln T + \beta_4 \ln U + \ln e \quad (\text{Eq.5})$$

where I is the carbon emissions in each province; P is the population; A is wealth, expressed by per capita GDP; T is energy intensity (Total energy consumption /GDP); U is the level of urbanization, expressed by the ratio of urban population to permanent population; β_1 , β_2 , β_3 and β_4 are elastic coefficients.

(2) Prediction of multiple scenarios

Secondly, this paper uses STIRPAT model to forecast the future carbon emissions of Inner Mongolia, Qinghai, Shaanxi, Gansu, Shanxi, Henan, Ningxia, and Shandong provinces. The specific formula is as follows:

$$I = \exp(a + \beta_1 \ln P + \beta_2 \ln A + \beta_3 \ln T + \beta_4 \ln U) \quad (\text{Eq.6})$$

Based on the historical data, this research adopts the above formula to simulate the historical carbon emissions in 8 provinces, and then regression the simulated values with the true values. If the results show that the model fits well, it indicates that it is doable to use the above model to predict the carbon emissions in 8 provinces from 2030 to 2100. Then, the data of influencing factors of 8 provinces from 2030 to 2100 can be brought into formula (6) to get the carbon emissions of 8 provinces from 2030 to 2100.

Land use dynamic attitude

Land use dynamic index is an indicator to measure the average annual change amplitude of regional land use, which can be spanned into land use dynamic attitude of single land use type (SLDI) and comprehensive land use dynamic attitude (CLDI) (Wu et al., 2014; Liu et al., 2021).

The SLDI was used to characterize the annual change of a certain land use type area in a certain period of time. The formula is:

$$SLDI_i = \frac{A_{ni} - A_{mi}}{A_{mi} \cdot T} \times 100\% \quad (\text{Eq.7})$$

where A_{mi} and A_{ni} respectively represent the area of the i type of land use at the starting year (m) and the end year (n) of the research period.

The CLDI was used to characterize the annual changes of all land use types in a certain period of time. The formula is:

$$CLDI = \left(\frac{\sum_{i=1}^k \Delta A_{mi}}{2 \sum_{i=1}^k A_{mi} T} \right) / T \times 100\% \quad (\text{Eq.8})$$

where A_{mi} represents the area of the i type of land use at the starting of the study period; ΔA_{mi} is the absolute value of the area converted from type i to non-type i in the study period.

Coefficient of variation and Theil index

The coefficient of variation (CV) reflects the relative dispersion, and it is an vital indicator to measure regional differences between years (Pan et al., 2020). The Thiel index (TI) measures the relative disparity between regions. In this study, CV is employed to measure the regional difference degree of carbon balance, and TI is used to measure the overall difference of carbon balance (Shen et al., 2023). The calculation formulas are as follows:

$$CV = \frac{1}{\bar{y}} \sqrt{\frac{\sum_{i=1}^n (y_i - \bar{y})^2}{n}} \quad (\text{Eq.9})$$

$$T = \frac{1}{n} \sum_{i=1}^n \frac{y_i}{\bar{y}} \log \left(\frac{y_i}{\bar{y}} \right) \quad (\text{Eq.10})$$

where n is the number of research units; y_i is the net carbon emission of region i , and \bar{y} is the average net carbon emission of region n .

Results

Changes of carbon budget during 2000-2020

Changes of carbon sequestration during 2000-2020

The carbon sequestration in the YRB shows an overall trend of fluctuating and increasing during 2000-2020 (Fig. 3a). The change of total carbon emissions can be spanned into four stages, namely, the stage of rapid increase from 2000 to 2007, the stage of decreasing fluctuation from 2008 to 2014, the stage of sharp increase from 2015 to 2016, and the stage of steady growth from 2017 to 2020. From the perspective of provinces (Fig. 3b-3i), Inner Mongolia has the highest carbon sealed stock, which is much higher than other provinces. This was followed by Qinghai, Shaanxi, Gansu, and Shaanxi, all of which had more than 2 million tons of carbon locked up. Henan, Shandong, and Ningxia have the lowest carbon storage. From the perspective of time evolution of carbon

storage in various provinces, Inner Mongolia, Shanxi, and Gansu showed an increasing trend, Shandong showed a decreasing trend, Qinghai and Ningxia showed an inverted U-shaped trend, Henan showed an M-shaped trend, and Shaanxi showed an N-shaped trend.

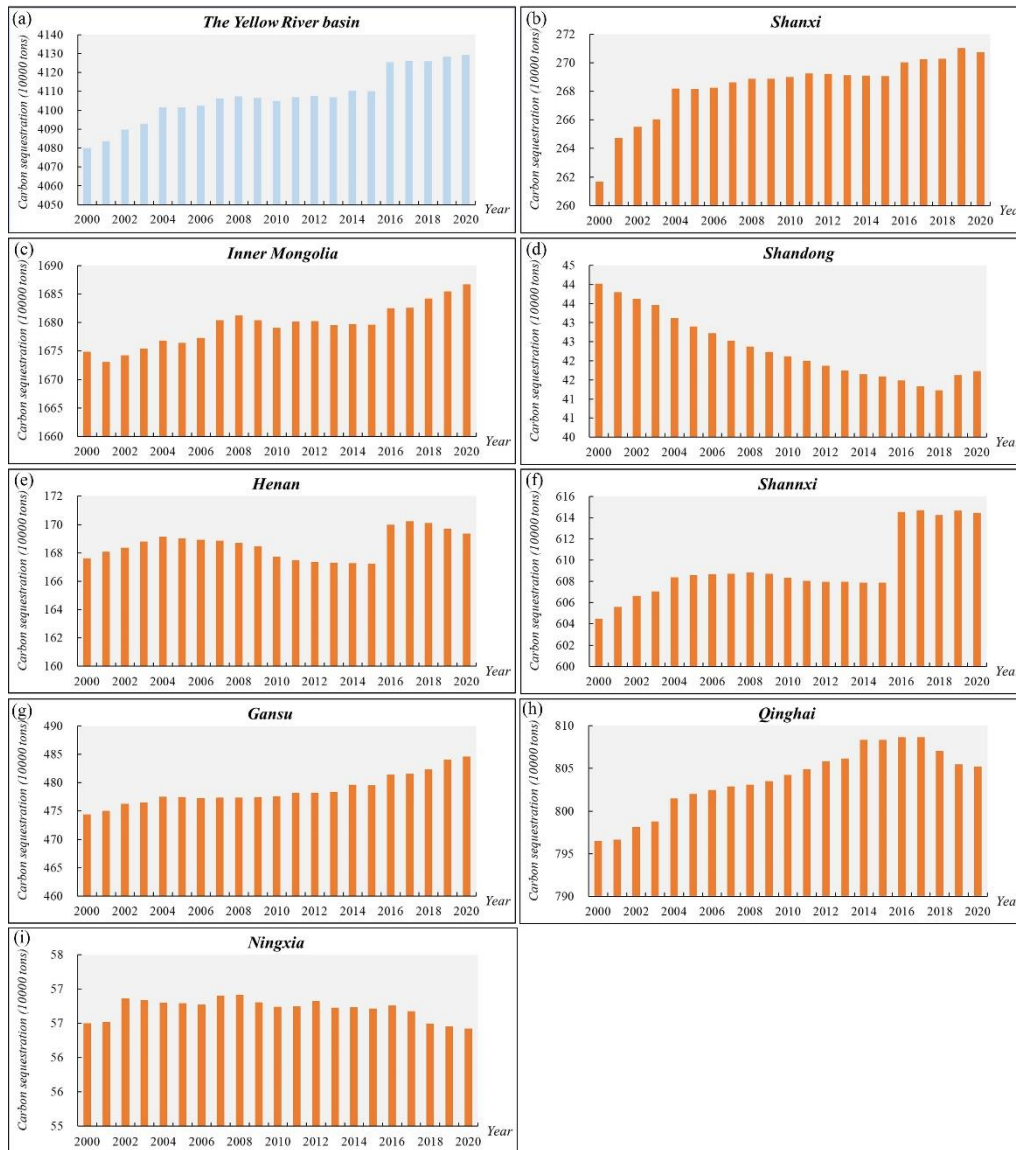


Figure 3. Time changes of carbon sequestration stocks in study area (a) and provinces (b-i) from 2000 to 2020

Changes of carbon emissions during 2000 to 2020

The general carbon emission shows a tendency of fluctuation and increase during 2000-2020 (Fig. 4). The evolution of carbon emissions can be spanned into three stages: the speedy growth of total carbon emissions from 2000 to 2011, the slow growth of carbon emissions from 2012 to 2016, and the speedy growth of carbon emissions from 2017 to 2020. Carbon emissions in the YRB were 5.9 million tons in 2000 and 30.28 million tons in 2020, an increase of 4.13 times compared with 2000 in 2020. This is mainly due to rapid population growth (up nearly 9% in 2020 compared to 2000), rapid expansion of

urbanization (up nearly 110%), rapid growth of gross domestic product (up nearly 900%), and rapid growth of total energy consumption (up nearly 290%). By province, Shandong and Inner Mongolia have the highest total carbon emissions, followed by Shanxi, Henan and Shaanxi, and Ningxia and Qinghai have the lowest carbon emissions. From the point of view of the time evolution of each province, Shandong, Shanxi, and Shaanxi maintain the trend of fluctuation and rise, and the growth rate is fast. Inner Mongolia is the fastest growing province in terms of carbon emissions, rising from fourth to second in 2011. The carbon emissions in Gansu and Qinghai showed a slow growth tendency in time series. Henan's carbon emissions peaked in 2011 and have fluctuated since then.

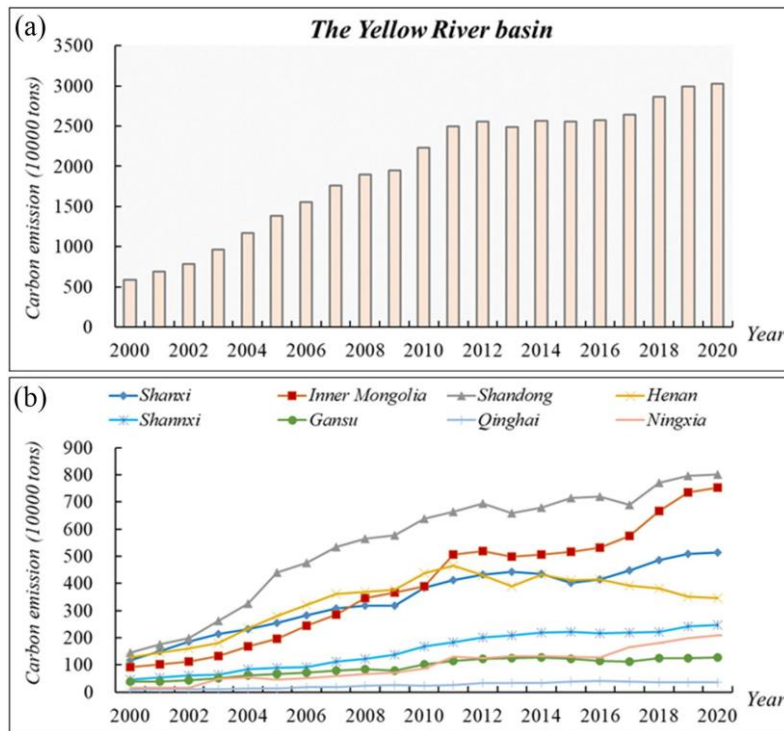


Figure 4. Carbon emission changes in study area (a) and provinces (b) from 2000 to 2020

Changes of carbon balance in the YRB from 2000 to 2020

As can be seen from Figure 5, net carbon budget in the YRB is negative (carbon emissions are less than carbon storage) and show an overall trend of fluctuation and increase in time series. The temporal variation of net carbon budget can be spanned into two stages: the rapid increase stage from 2000 to 2011, and the slow increase stage from 2012 to 2020. Overall, the pressure of carbon balance gradually increases from 2000 to 2020, which is mainly due to the huge carbon emission caused by economic development. In term of net carbon budget by provinces (Fig. 6), the net carbon emissions of Inner Mongolia, Qinghai, Shaanxi, and Gansu are negative (carbon sink region), and the net carbon budget of Shandong are positive (carbon source region). Henan, Shanxi, and Ningxia changed from carbon sink region to carbon source region in 2003, 2006 and 2007 respectively. In term of time evolution of net carbon budget in each province, Henan's net carbon budget peaked in 2011 and then showed a gradual decline. Net carbon budget in Inner Mongolia, Qinghai, Shaanxi, Gansu, Shandong, Shanxi, and Ningxia all showed a slow increase.

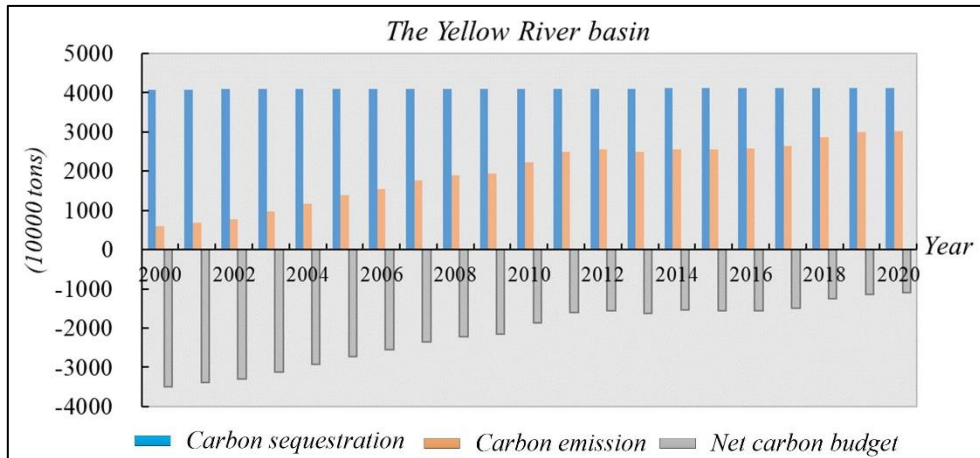


Figure 5. Time changes of net carbon budget during 2000 to 2020

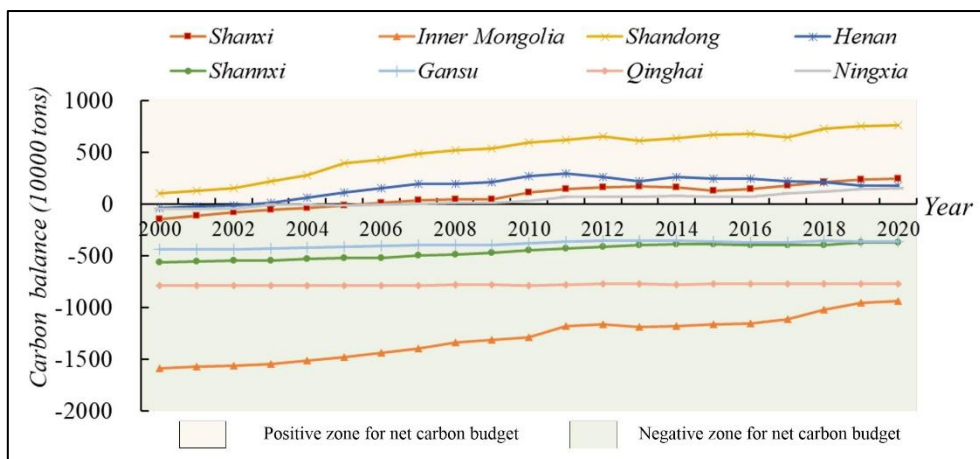


Figure 6. Time changes of provincial of net carbon budget during 2000-2020

Simulation of carbon budget from 2030 to 2100 under different SSP scenarios

Future land use pattern under SSP1-5 scenario

The spatial characteristic of land use in the YRB during 2030-2100 under the SSP scenario is as follows (Fig. 7): (1) SSP1 scenario. From 2030 to 2100, cultivated land was primarily spreaded over central Shaanxi, Shanxi, Henan, Shandong, and southeast Inner Mongolia; forest land was mainly distributed in the Greater Khingan Mountains, Qinling Mountains, Liupan Mountains, and Taihang Mountains; grassland was primarily spread over the Inner Mongolia Plateau and Qinghai Province. Construction land was primarily distributed in the Middle and Lower Reaches of the Yellow River Plain. Bare land and desert are mainly distributed in western Inner Mongolia, western Gansu, and northwestern Qinghai. A comparison of the spatial characteristic of land use shows that under the SSP1 scenario, the woodland area in the Greater Khingan Mountains, the central Shaanxi Plateau, the Qinling Mountains, Xiaoshan Mountains and Funiu Mountains have significantly increased, and the woodland connectivity has been enhanced significantly during 2030-2100 (Fig. 8). The bare land area of western Gansu and central and western Inner Mongolia Plateau has expanded significantly. The cultivated land area in the central

part of Inner Mongolia Plateau and the central and northern part of Ningxia is less, while the farmland area in the northern part of northern Shaanxi Plateau is increased to a certain extent.

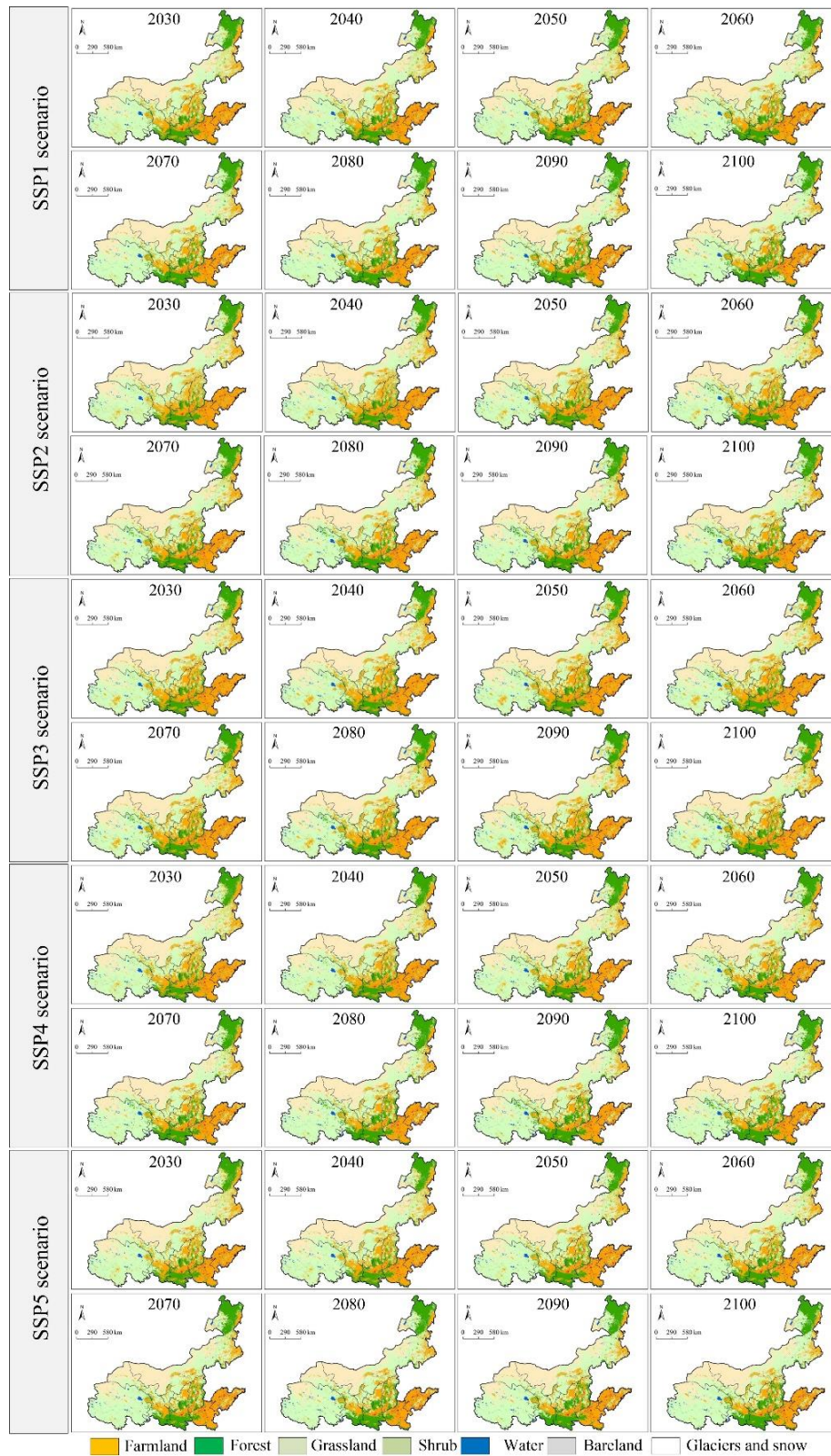


Figure 7. Landuse pattern from 2030 to 2100 under the SSP1-5 development scenario

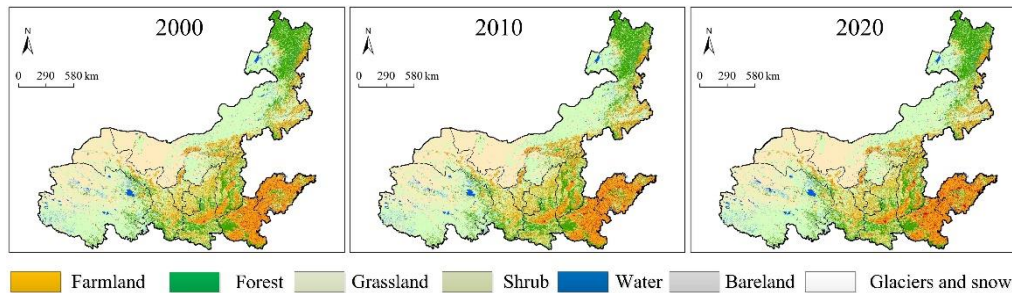


Figure 8. Landuse pattern from 2000 to 2020

(2) SSP2 scenario. A comparison of the spatial characteristic of land use shows that under the SSP2 scenario, the woodland areas in the Great Khingan Mountains, the central part of the Northern Shaanxi Plateau, the Qinling Mountains, the Xiaoshan Mountains, and the Funiu Mountains have all increased significantly, and the woodland connectivity has been enhanced significantly from 2030 to 2100. The bare land area in western Gansu, the midwest and northeast of Inner Mongolia Plateau were significantly expanded, while the grassland area was significantly less, indicating that the land degradation trend had been intensified. The farmland area in the central part of Inner Mongolia Plateau and the central and northern part of Ningxia is less, while the farmland area in the Northern Shaanxi Plateau is increased to a certain extent.

(3) SSP3 scenario. In comparison with the spatial characteristic of land use shows that under the SSP3 scenario, the forest land area and connectivity in the Daxingan Mountains, the central Shaanxi Plateau, the Qinling Mountains, the Xiaoshan Mountains, and the Funiu Mountains have all increased significantly from 2030 to 2100. The trend of land degradation has intensified in western Gansu, central and western Inner Mongolia Plateau and northeastern regions. Compared with SSP1 and SSP2 scenarios, the cultivated land area in northern Shaanxi Plateau, Guanzhong Basin, central and western Shanxi and southern Qinghai increased more during 2030-2100 under SSP3 scenario, and the construction land expansion in Henan and Shandong was significant.

(4) SSP4 scenario. The spatial characteristic of land use in 2030-2100 under the SSP4 scenario has significantly changed compared with the historical years. Compared with SSP1, SSP2 and SSP3 scenarios, under SSP4 scenario, the area of forestland and grassland in central Shaanxi Plateau, Taihang Mountains in central Shanxi, Taishan and Mengshan Mountains in Shandong will increase greatly during 2030-2100, while the area of farmland in Ordos Plateau in central Inner Mongolia, Horqin Plain and Songliao Plain in eastern Inner Mongolia will decrease relatively. The area of forestland and grassland in the northeast of Qinghai was reduced.

(5) SSP5 scenario. The area of farmland expanded visibly in Guanzhong Basin, Henan Plain and Shandong Province. Compared with the SSP-4 scenario, under the SSP5 scenario, the cultivated land area in Longnan region, Guanzhong Basin, central and western Shanxi, central Henan Plain, and central Shandong region will expand more significantly from 2030 to 2100. The expansion of farmland area is more evident in central Shanxi, Guanzhong Basin, Henan Plain, northern, and coastal areas of Shandong Province. Forest and grassland areas in the central and eastern parts of Qinghai, Ordos Plateau, Horqin Plain, Songliao Plain, and the Luliang and Taihang Mountains in central Shanxi have decreased sharply.

In terms of future land use dynamic attitude, the CLDI in the YRB under five development scenarios is 0.0654, 0.0608, 0.0348, 0.0734 and 0.0708, respectively, among which the CLDI in SSP3 scenario is the smallest, and that in SSP4 scenario is the largest. From the perspective of SLDI (Table 2), 7 periods under SSP5 scenario have the largest fluctuation in time series, while the SSP1 scenario is the most stable. The land use change processes in SSP2, SSP4 and SSP5 scenarios are basically the same, that is, the land use change processes are inverted U-shaped. The SSP1 and SSP3 scenarios are "M" type and "W" type change processes respectively.

Table 2. The SLDI from 2030 to 2100 under the SSP1-5 scenario

Time period	SLDI (%)				
	SSP1	SSP2	SSP3	SSP4	SSP5
2030-2040	0.0531	0.0365	0.0893	0.0513	0.0251
2040-2050	0.0747	0.0381	0.0380	0.0906	0.1237
2050-2060	0.0741	0.0732	0.0453	0.1259	0.0814
2060-2070	0.0685	0.1057	0.0443	0.1022	0.0857
2070-2080	0.0403	0.0987	0.0437	0.0660	0.0670
2080-2090	0.0711	0.0613	0.0296	0.0481	0.0633
2090-2100	0.0756	0.0547	0.0211	0.0488	0.0605
2030-2100	0.0654	0.0608	0.0348	0.0734	0.0708

Multi-scenario simulation of carbon sequestration

From the perspective of carbon sequestration of provinces (Fig. 9), the order of carbon sequestration of all provinces under the SPP1-5 scenario is the same, namely Inner Mongolia, Qinghai, Shaanxi, Gansu, Shanxi, Henan, Ningxia and Shandong. Among them, Inner Mongolia's carbon storage is more than 14 million tons, which has an absolute advantage compared with other provinces. The carbon sequestration capacity of Qinghai, Shaanxi and Gansu is more than 4.5 million tons, which is the backbone of increasing carbon sequestration in the YRB. Henan and Shanxi have more than 1.5 million tons of carbon sequestration, which also plays a vital role in increasing the regional carbon sink. The carbon storage in Ningxia and Shandong is less than 600,000 tons, and the carbon storage is obviously insufficient. Under different development scenarios, different provinces show the time evolution trend of travel alienation. In detail, under the SPP1-5 scenario, the carbon storage of Qinghai, Shaanxi, Gansu, Shanxi, Inner Mongolia, Ningxia and Shandong all showed a slow rise from 2030 to 2100, but the growth rate of SSP1, SSP2 and SSP4 scenarios was higher than that of SSP3 and SSP5 scenarios. Under SSP1, SSP2, SSP4 and SSP5 scenarios, the carbon sequestration stock in Henan Province showed a tendency of first decreasing and then increasing, while under SSP3 scenario, it showed a trend of slow decreasing.

According to the differences of carbon storage in different provinces (Fig. 10): (1) Under the SSP1-5 scenario, the carbon storage of Gansu, Shaanxi and Shanxi showed a steady increase trend during the simulation period. (2) Carbon storage in Inner Mongolia and Shandong under SSP1, SSP4 and SSP5 scenarios was significantly higher than that under SSP2 and SSP3 scenarios, showing an "S" -shaped development trend of first rapid increase and then slow increase during the simulation period. (3) Under the SSP1-5 scenario, the temporal evolution of carbon uptake in Qinghai showed phased

characteristics. The total carbon storage of Qinghai under SSP1, SSP4 and SSP5 scenarios from 2030 to 2040 is greater than that under SSP2 and SSP3 scenarios, the carbon uptake of SSP2 scenarios from 2040-2060 gradually exceeds that of SSP1 and SSP5 scenarios, and the carbon uptake of SSP3 scenarios from 2060 to 2100 exceeds that of SSP1 and SSP5 scenarios. The SSP2 scenario gradually catches up with the SSP4 scenario. (4) The carbon storage in Ningxia showed an "S" -shaped trend under SSP1, SSP2, SSP4 and SSP5 scenarios, and a "U" -shaped trend under SSP3 scenario, which showed a rapid decline at first and then a slow increase. (5) The total carbon storage in Henan showed a U-shaped change process of rapid decline first and then rapid increase under the SSP1, SSP2, SSP4 and SSP5 scenarios, while it showed a slow decline trend under the SSP3 scenario.

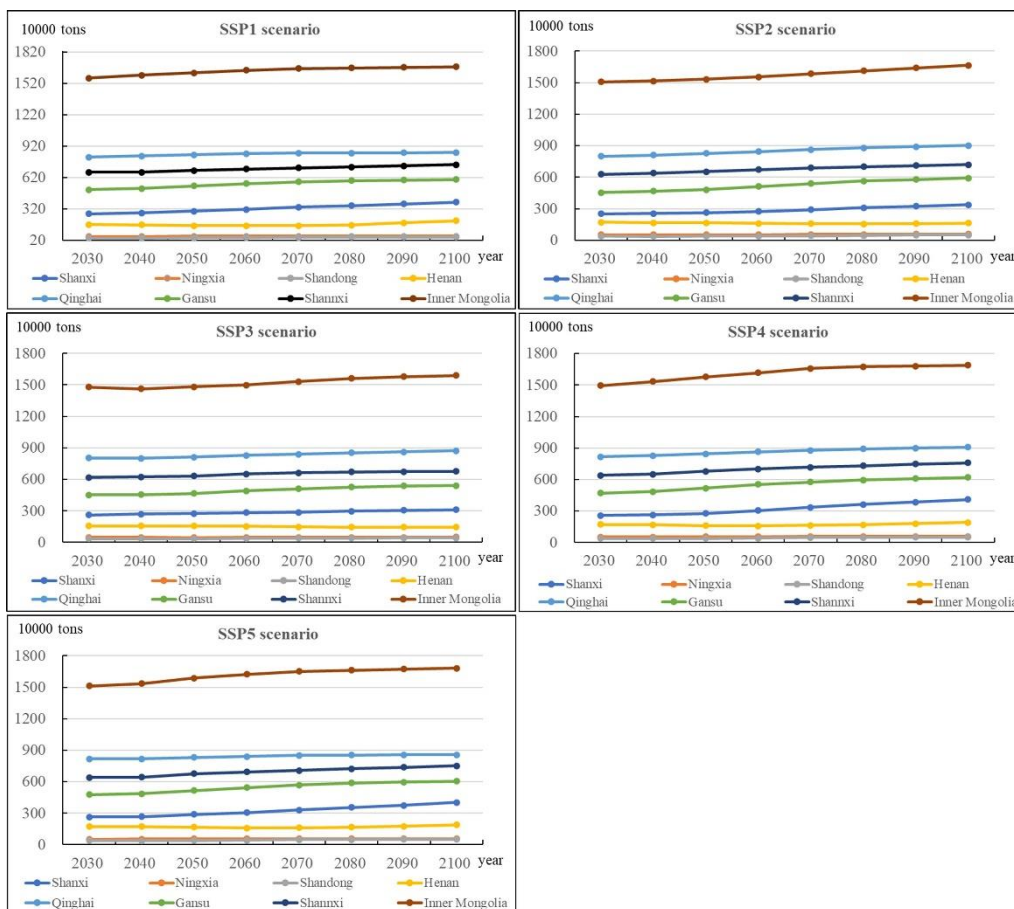


Figure 9. Temporal changes of carbon storage during 2030-2100 under the SSP1-5 scenario

Multi-scenario simulation of carbon emissions

(1) Regression analysis

Firstly, SPSS was used to conduct multiple regression analysis on Inner Mongolia, Gansu, Henan, Shandong, Shaanxi, Qinghai, Shanxi and Ningxia, and it was found that all 8 models had severe multicollinearity. Therefore, so as to eliminate the impact of multicollinearity, ridge regression method was adopted in this paper for regression analysis, and the results are shown in Table 3.

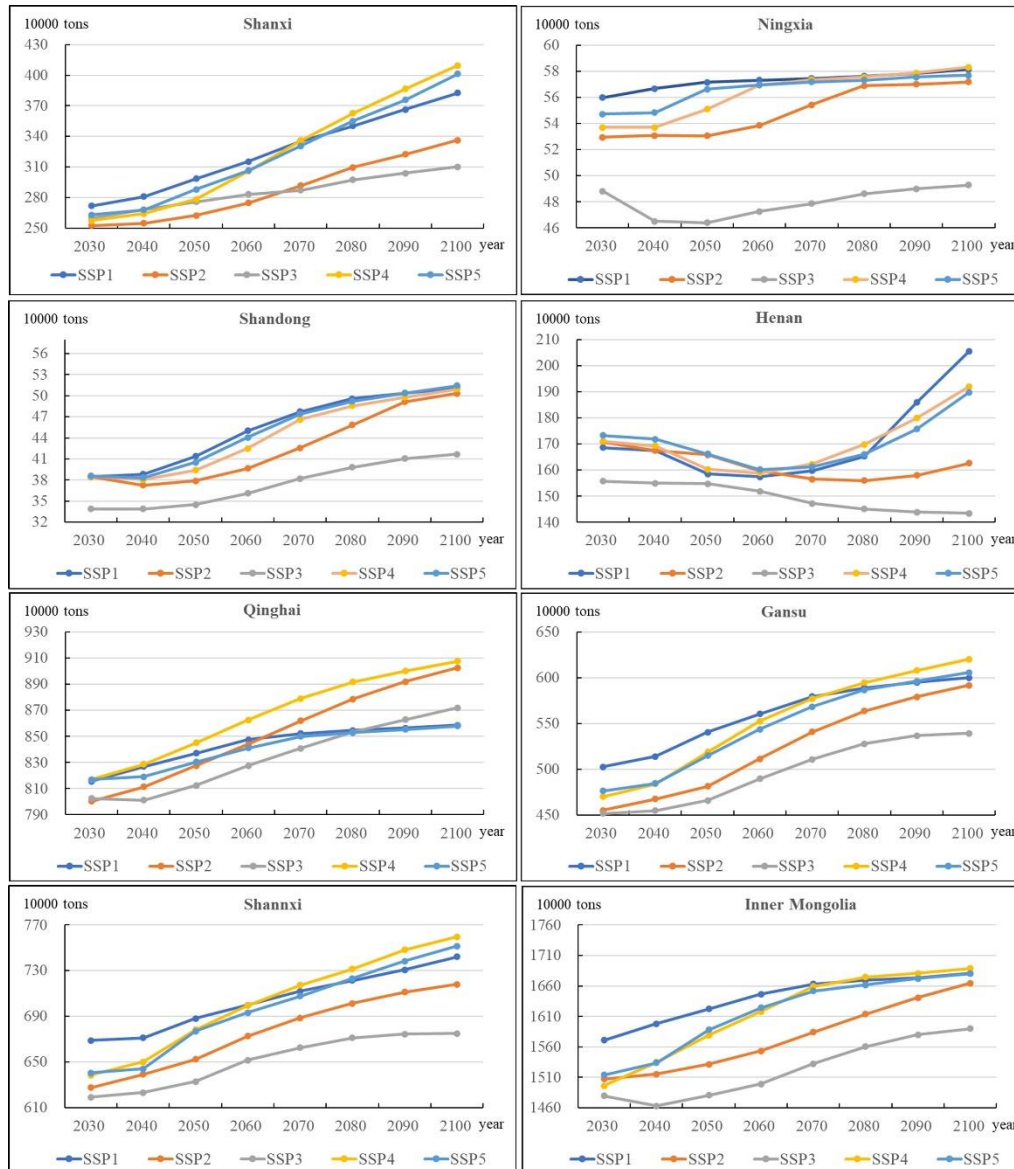


Figure 10. Temporal changes of provincial carbon sequestration stocks during 2030-2100 under the SSP1-5 scenario

As can be seen from *Table 3*, each model variable has a high significance level, and the F statistic passes the significance level test of 1%. Therefore, the models built by the eight provinces can superior explain the relationship between carbon emissions and influencing factors, and the specific forms of each model are shown in *Table 4*. According to the regression coefficient (*Table 4*), the increase of $\ln P$, $\ln A$, $\ln T$, and $\ln U$ will promote the increase of carbon emissions. Among them, the $\ln P$ factor has the biggest effect on carbon emissions, followed by the $\ln U$ factor.

(2) Multi-scenario simulation of carbon emissions

The regression models constructed by eight provinces (*Table 4*) can well account for the relationship between carbon emissions and influencing factors, so the STIRPAT model (*Table 5*) is adopted in this study to predict the change of carbon emissions in eight provinces. First, eight models in *Table 5* were used to simulate the carbon emissions in

Inner Mongolia, Gansu, Henan, Shandong, Shaanxi, Qinghai, Shanxi and Ningxia in historical years, and the simulated values in historical years were compared with the real values in historical years, and the simulation accuracy was verified. As shown in *Figure 11*, by comparing the real value of carbon emissions from 2000 to 2020 with the simulated value, we find that the prediction model has a high degree of fit, with R^2 reaching more than 0.95. Hence, it is doable to use eight prediction models to forecast the carbon emissions in each province during 2030-2100.

Table 3. Analysis results of ridge regression model

Region	Variable	Nonnormalized coefficient	Standardization coefficient	t	P	R ²	Adjust R ²	F
Inner Mongolia	Constant	-60.186	-	-7.618	0.000***	0.984	0.980	230.06 (0.000***)
	lnP	7.167	0.253	7.246	0.000***			
	lnA	0.358	0.471	10.1	0.000***			
	lnT	0.156	0.085	1.691	0.112			
	lnU	1.559	0.321	13.208	0.000***			
Gansu	Constant	44.508	-	2.717	0.016**	0.963	0.953	97.50 (0.000***)
	lnP	-5.698	-0.201	-2.694	0.017**			
	lnA	0.302	0.522	10.293	0.000***			
	lnT	-0.342	-0.316	-6.692	0.000***			
	lnU	0.545	0.293	7.331	0.000***			
Henan	Constant	65.004	-	2.097	0.053*	0.796	0.741	14.60 (0.000***)
	lnP	-6.878	-0.2	-2.036	0.060*			
	lnA	0.36	0.684	7.208	0.000***			
	lnT	-0.007	-0.007	-0.075	0.941			
	lnU	0.049	0.044	0.404	0.692			
Shandong	Constant	-28.777	-	-5.764	0.000***	0.922	0.901	44.36 (0.000***)
	lnP	3.036	0.219	5.703	0.000***			
	lnA	0.353	0.446	10.081	0.000***			
	lnT	0.443	0.227	3.12	0.007***			
	lnU	0.97	0.373	9.222	0.000***			
Shannxi	Constant	24.298	-	1.289	0.217	0.975	0.968	144.25 (0.000***)
	lnP	-3.272	-0.107	-1.403	0.181			
	lnA	0.384	0.61	9.681	0.000***			
	lnT	-0.154	-0.108	-1.611	0.128			
	lnU	0.963	0.347	8.698	0.000***			
Qinghai	Constant	-13.657	-	-1.964	0.068*	0.972	0.964	129.21 (0.000***)
	lnP	2.173	0.202	1.916	0.075*			
	lnA	0.516	0.768	6.662	0.000***			
	lnT	-0.25	-0.143	-1.25	0.230			
	lnU	-0.512	-0.141	-1.394	0.184			
Shanxi	Constant	5.053	-	0.733	0.475	0.958	0.947	85.255 (0.000***)
	lnP	-0.674	-0.08	-0.755	0.462			
	lnA	0.284	0.519	6.423	0.000***			
	lnT	-0.113	-0.134	-1.584	0.134			
	lnU	0.907	0.389	3.998	0.001***			
Ningxia	Constant	-25.983	-	-6.045	0.000***	0.934	0.916	52.65 (0.000***)
	lnP	3.056	0.258	5.103	0.000***			
	lnA	0.36	0.347	9.571	0.000***			
	lnT	0.262	0.098	1.192	0.252			
	lnU	1.757	0.408	7.563	0.000***			

Note: ***, ** and * represent significance levels of 1%, 5% and 10% respectively

Table 4. Regression model formulas constructed by 8 provinces

Province	Model formula
Inner Mongolia	$\ln I = -60.186 + 7.167 \ln P + 0.358 \ln A + 0.156 \ln T + 1.559 \ln U$
Gansu	$\ln I = 44.508 - 5.698 \ln P + 0.302 \ln A - 0.342 \ln T + 0.545 \ln U$
Henan	$\ln I = 65.004 - 6.878 \ln P + 0.36 \ln A - 0.007 \ln T + 0.049 \ln U$
Shandong	$\ln I = -28.777 + 3.036 \ln P + 0.353 \ln A + 0.443 \ln T + 0.97 \ln U$
Shannxi	$\ln I = 24.298 - 3.272 \ln P + 0.384 \ln A - 0.154 \ln T + 0.963 \ln U$
Qinghai	$\ln I = -13.657 + 2.173 \ln P + 0.516 \ln A - 0.25 \ln T - 0.512 \ln U$
Shanxi	$\ln I = 5.053 - 0.674 \ln P + 0.284 \ln A - 0.113 \ln T + 0.907 \ln U$
Ningxia	$\ln I = -25.983 + 3.056 \ln P + 0.36 \ln A + 0.262 \ln T + 1.757 \ln U$

Table 5. Carbon emission prediction models for 8 provinces

Province	Model formula
Inner Mongolia	$I = \exp(-60.186 + 7.167 \ln P + 0.358 \ln A + 0.156 \ln T + 1.559 \ln U)$
Gansu	$I = \exp(44.508 - 5.698 \ln P + 0.302 \ln A - 0.342 \ln T + 0.545 \ln U)$
Henan	$I = \exp(65.004 - 6.878 \ln P + 0.36 \ln A - 0.007 \ln T + 0.049 \ln U)$
Shandong	$I = \exp(-28.777 + 3.036 \ln P + 0.353 \ln A + 0.443 \ln T + 0.97 \ln U)$
Shannxi	$I = \exp(24.298 - 3.272 \ln P + 0.384 \ln A - 0.154 \ln T + 0.963 \ln U)$
Qinghai	$I = \exp(-13.657 + 2.173 \ln P + 0.516 \ln A - 0.25 \ln T - 0.512 \ln U)$
Shanxi	$I = \exp(5.053 - 0.674 \ln P + 0.284 \ln A - 0.113 \ln T + 0.907 \ln U)$
Ningxia	$I = \exp(-25.983 + 3.056 \ln P + 0.36 \ln A + 0.262 \ln T + 1.757 \ln U)$

The simulation results show (Fig. 12) that the carbon emissions of eight provinces during 2030-2100 show different evolutionary characteristics in terms of time series, and the same province shows great differences in different development scenarios. The general carbon emissions in Inner Mongolia, Qinghai and Shandong showed a downward trend during 2030-2100, with a faster decline during 2030-2060, and a slow decline during 2060-2100. The total carbon emissions in Gansu, Henan, Shaanxi, Shanxi and Ningxia showed an overall upward trend, and the carbon emissions in different scenarios showed a slow upward trend during 2030-2070, and a rapid upward trend during 2070-2100.

The carbon emissions of Gansu, Henan, Shaanxi, Shanxi and Ningxia are the lowest under SSP2 and SSP3, and the highest under SSP4 and SSP5. The carbon emissions in Inner Mongolia, Qinghai and Shandong reached the highest under SSP2 and SSP3 scenarios and reached the lowest under SSP1 and SSP4 scenarios.

Multi-scenario simulation of carbon balance

(1) Evolution of carbon balance in the YRB from 2030 to 2100

As shown in Fig. 13, under the SSP1-5 scenario, net carbon emissions in the YRB during 2030-2100 showed a fluctuating evolution tendency. From 2030 to 2080, under the SSP1-5 scenario, the carbon uptake of the YRB is less than the carbon emission of energy, so it is a net carbon source area. From 2080 to 2100, under the SSP1-5 scenario, carbon uptake in the Yellow River Basin is greater than energy carbon emissions, so it is a net carbon sink area. Under the SSP4 scenario, the Yellow River Basin changes from a net carbon source area to a net carbon sink area first, followed by the SSP5 and SSP1

scenarios. The SSP2 scenario changes to a net carbon sink area in 2090, while the SSP3 scenario remains a net carbon source area from 2030 to 2100. The sharp increase of carbon emissions and the slow increase of carbon sequestration stock lead to the extremely unbalanced carbon budget in the Yellow River Basin. Therefore, effective measures should be taken to enhance the terrestrial carbon absorption capacity and reduce the pressure of carbon emissions.

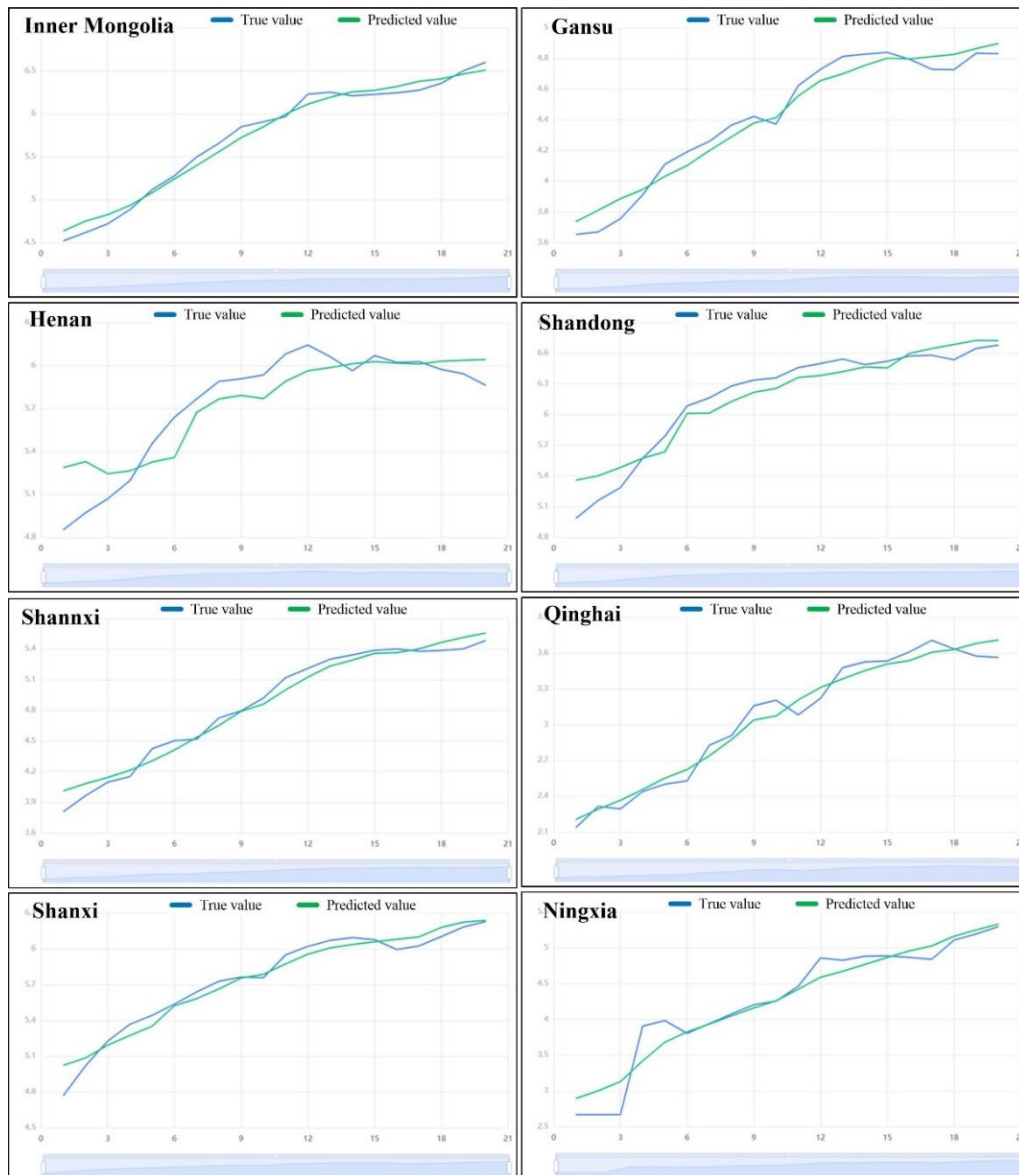


Figure 11. Comparison of simulated values of the forecast model with historical values

Further, we use the coefficient of variation (CV) and Theil index (TI) to analyze the regional differences of carbon budget in the provinces of the YRB. As shown in *Table 6*, the CV (highly variable state, $CV > 0.35$) and TI (both greater than 0.2) of the provincial carbon budget in the YRB during 2030-2100 are both large, indicating that the regional differences of the provincial carbon budget in the YRB during 2030-2100 under the development scenario of SSP1-5 are large. Compared among different scenarios, SSP3

scenario has the smallest regional difference, followed by SSP4 and SSP5 scenarios, and SSP1 and SSP2 scenarios have the largest regional difference. In terms of time series, the regional differences of provincial carbon budget under the development scenarios of SSP1, SSP3, SSP4 and SSP5 all showed a change process of first increasing and then decreasing, while the regional differences of SSP2 gradually increased.

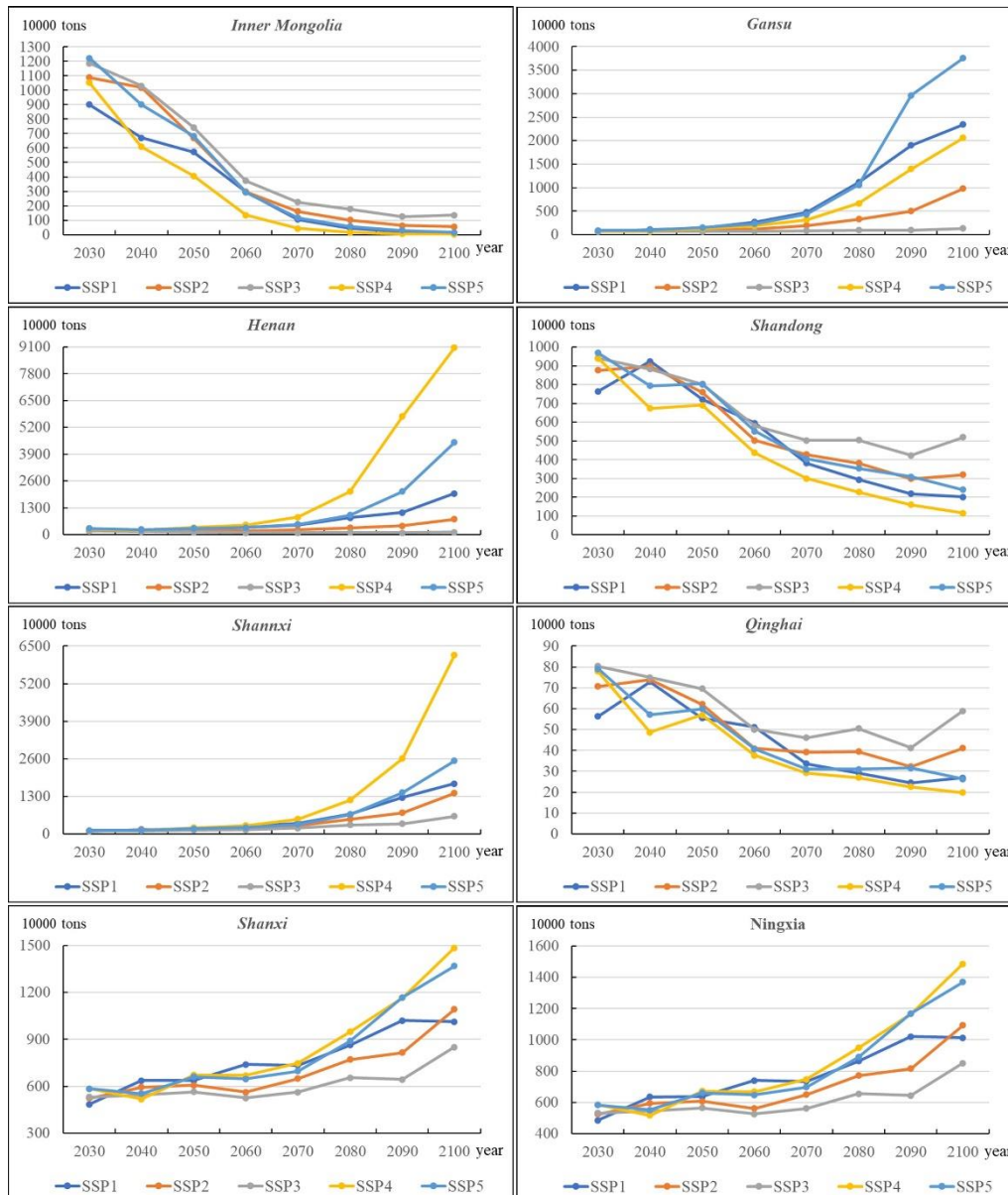


Figure 12. Carbon emission projections of eight provinces during 2030-2100 under the SSP1-5 scenario

(2) Change of provincial carbon balance during 2030-2100

Under the SSP1-5 scenario, net carbon emissions of eight provinces during 2030-2100 show significant temporal evolution characteristics (Fig. 14). In the short to medium term (2030-2070), the overall net carbon emissions of the eight provinces under the SSP1-5 scenario show a slow trend of decline (the net carbon emissions of Inner Mongolia and

Qinghai gradually decrease). In the long-term future (2070-2100), the net carbon emissions of the eight provinces under the SSP1-5 scenario will show an overall upward trend. Under SSP1, SSP2, SSP4 and SSP5 scenarios, Shaanxi and Gansu gradually changed from carbon sink region to carbon source region. Under SSP3 scenario, Shaanxi is gradually transformed from carbon sink region to carbon source region.

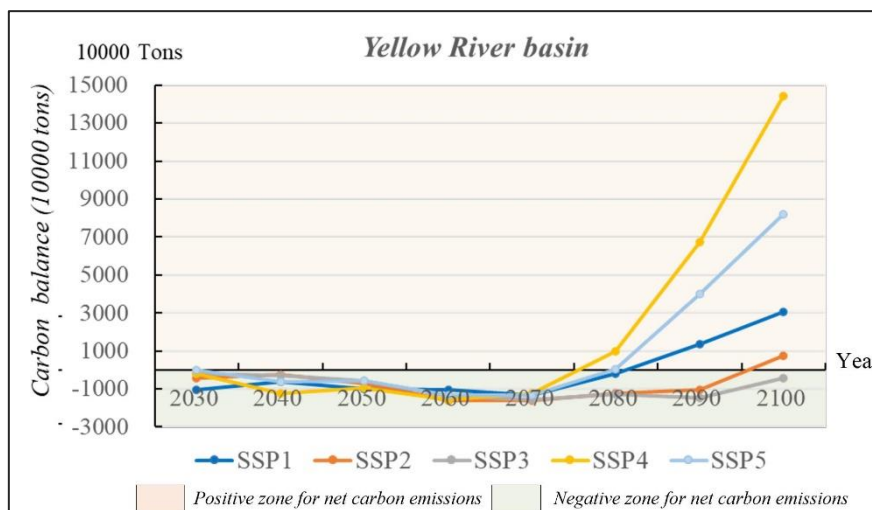


Figure 13. Time changes of net carbon emissions during 2030 to 2100 under the SSP1-5 scenario

Table 6. Regional differences of provincial carbon budget during 2030-2100 under the SSP1-5 scenario

Scene	Parameter	2030	2040	2050	2060	2070	2080	2090	2100
SSP1	CV	0.643	0.694	0.803	0.936	1.168	1.172	0.840	0.844
	TI	0.232	0.266	0.348	0.425	0.586	0.542	0.312	0.365
SSP2	CV	0.615	0.665	0.767	0.853	0.901	0.992	1.162	1.287
	TI	0.216	0.252	0.334	0.368	0.380	0.433	0.550	0.633
SSP3	CV	0.594	0.649	0.734	0.730	0.717	0.680	0.681	0.623
	TI	0.205	0.245	0.331	0.287	0.266	0.240	0.237	0.208
SSP4	CV	0.622	0.743	0.875	1.070	0.902	0.579	0.459	0.500
	TI	0.220	0.296	0.399	0.530	0.357	0.183	0.143	0.164
SSP5	CV	0.617	0.690	0.780	0.934	1.131	1.051	0.700	0.604
	TI	0.216	0.267	0.337	0.425	0.555	0.443	0.267	0.210

From each scenario: (1) SSP1 scenario. In the short to medium term (2030-2070), the net carbon emissions of eight provinces will decline gradually, and the number of negative and positive regions will remain basically unchanged. The carbon sources include Inner Mongolia, Qinghai, Shaanxi and Gansu, and the carbon sinks include Henan, Shanxi, Ningxia and Shandong and other central and eastern provinces. In the long run (2070-2100), the net carbon emissions of Inner Mongolia, Qinghai, Ningxia, and Shandong will decline gently, Shanxi showed a fluctuating upward trend, while the net carbon emissions of Gansu, Shaanxi and Henan increased rapidly. (2) SSP2 scenario.

Under the SSP2 scenario, the net carbon emissions of Inner Mongolia, Qinghai, Ningxia and Shandong decreased slowly during 2030-2100, while the net carbon emissions of Gansu, Shaanxi, Shanxi and Henan increased. (3) SSP3 scenario. Under the SSP3 scenario from 2030 to 2100, the net carbon emissions of Inner Mongolia, Qinghai, Gansu, Shaanxi and Henan will decrease slowly, Shandong will decrease first and then increase, Shanxi will fluctuate and increase, and Ningxia will have a certain increase. (4) SSP4 and SSP5 scenarios. The net carbon emissions of Inner Mongolia, Qinghai Province and Shandong province during 2030-2100 will decrease to some extent, which is consistent with other scenarios. However, the rapid growth of net carbon emissions in Henan, Gansu, Shanxi and Shaanxi from 2070 to 2100, may be related to the pressure on resource load and the increase in energy consumption caused by economic and population development in these four provinces.

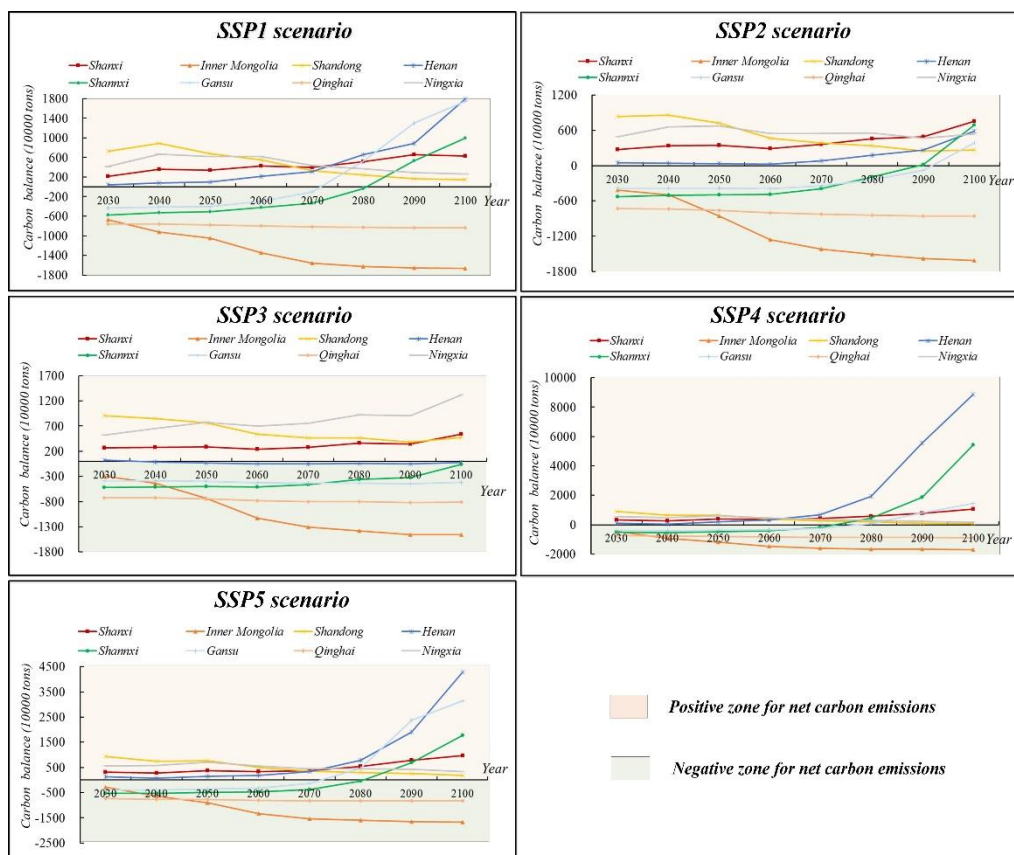


Figure 14. Time evolution of provincial net carbon emissions during 2030 to 2100 under SSP1-5 scenario

In general, Inner Mongolia and Qinghai maintain a good low-carbon development path under SSP1, SSP2 and SSP4 scenarios, Ningxia and Shandong maintain a good low-carbon development path under SSP1 and SSP2 scenarios, and Shanxi maintains a good low-carbon development path under SSP1 and SSP3 scenarios. Gansu, Shaanxi and Henan maintain a good low-carbon development path under the SSP3 scenario. Under the SSP4 and SSP5 scenarios, the net carbon emissions of Henan, Shaanxi, Gansu and Shanxi will increase rapidly in the future long-term period (2070-2100), and the economic development is relatively extensive.

Discussion

Status and changes of land use and carbon budget

From the perspective of land use pattern and its changes, from 2000 to 2020, forest land and grassland in the Yellow River Basin are mainly distributed in Inner Mongolia, Qinghai, Shaanxi, Gansu and Shaanxi, cultivated land and construction land are mainly distributed in Henan, Shanxi, Shandong and Ningxia, and unused land is mainly distributed in Inner Mongolia, Gansu and Ningxia. This shows that land use patterns are adapted to location, climate, and topographic environment (Li et al., 2021; Shen et al., 2023). In terms of carbon sequestration stock, since carbon sequestration stock is mainly closely related to land use changes such as forest land, grassland, water area and cultivated land (Wang et al., 2021), the spatial distribution of carbon sequestration stock in the Yellow River Basin is higher in Inner Mongolia, Qinghai, Shaanxi, Gansu and Shaanxi, while lower in Henan, Shandong, Shanxi and Ningxia. This is the same as the results of VanHoek et al. (2021) and Zhang et al. (2023). In terms of carbon emissions, energy consumption carbon emissions are mainly closely related to population, urbanization expansion, industrial development, etc., while the middle and lower reaches of the Yellow River Basin (Henan, Shandong, Shanxi and Inner Mongolia) are the main areas of population growth, urbanization expansion and economic development, so energy consumption carbon emissions are relatively high. In addition, the energy and raw material industries and industries with high energy consumption and high emissions in Inner Mongolia and Shanxi have a large stock and a high proportion, which is another major reason for high carbon emissions (Liu et al., 2021). In terms of multi-scenario prediction of carbon sequestration and carbon emissions, the study found that under the SSP1-5 scenario, the carbon stocks of Qinghai, Shaanxi, Gansu, Shanxi, Inner Mongolia, Ningxia and Shandong all showed a slow upward trend during 2030-2100, while the carbon emissions of Inner Mongolia, Qinghai and Shandong showed a general downward trend during 2030-2100. Gansu, Henan, Shaanxi, Shanxi and Ningxia showed an overall upward trend in carbon emissions. Similar evidence is provided by Liu et al. (2023), Xue et al. (2023), and He et al. (2022).

The regulation strategy of carbon balance

The Middle and Lower Reaches of the Yellow River (MLRYR) (Henan, Shandong, Shanxi, Shaanxi, and Inner Mongolia) are the most active regions in terms of regional economic development, which has spawned a relatively developed industrial system, complete infrastructure, and attracted population concentration and distribution, resulting in higher carbon emissions and carbon increment. On the one hand, carbon emissions from industrial energy consumption accounted for more than 66% of the general carbon emissions in the MLRYR, much higher than that of other industries; On the other hand, the carbon emissions from the consumption of domestic performance sources accounted for a relatively high proportion of the total, and the residential energy consumption still showed an increasing tendency year by year. There is a significant carbon deficit in the carbon budget in the MLRYR, so it is still a long way to achieve the carbon balance between carbon emissions and carbon absorption. In view of this, the specific regulation strategies are put forward: (1) Optimize the industrial structure and adjust the energy consumption structure. In terms of energy consumption carbon emissions, the leading carbon emission industry is industry, and coal and petroleum are the main fossil fuels consumed in industrial production and processing. Hence, in the future, the transition and

upgrading of traditional industries should be accelerated, and the proportion of traditional energy-consuming industries in industry should be reduced. We will intensify the development of emerging service industries and gradually optimize the low-carbon industrial structure. On the other hand, we should strengthen the adjustment of energy consumption structure and vigorously develop clean energy. (2) Promote low-carbon life and high-quality urbanization. Population and urbanization rate have a certain driving effect on the total energy carbon emissions in the YRB. Therefore, when controlling the increase of net carbon emissions, we should not only consider controlling the population size and optimizing the population structure, but also guide residents to moderate green consumption concept and build a low-carbon lifestyle. (3) Optimize land use patterns and enhance carbon uptake of ecological land. We should encourage the development of compact city and strengthen the construction of urban greening and ecological corridors. Urban planning should reduce the use mode of industrial land, residential land and transportation land with high carbon emission intensity, and adopt more reasonable land use scale, structure and layout to adjust urban carbon emission intensity. On the other hand, forestland, grassland, water and farmland, as important carriers of carbon absorption in terrestrial ecosystems, should be strengthened to protect these lands.

The Upper Reaches of the Yellow River (URYR) is an vital water supply and conservation region of the YRB, and it is also a key area for coordinating the ecological protection and management of the whole basin. Most of the region belongs to the plateau alpine climate area, and the vegetation types are mainly grassland and meadow, accounting for 64.23% of the general area, and the carbon sink potential is huge. Therefore, hoisting the carbon sequestration capacity of vegetation and decreasing carbon emissions are the keys to carbon balance development in the URYR. In view of this, specific control strategies are proposed: (1) Prevention and control of vegetation degradation in plateau ecosystem under the background of future climate change. Climate change has further weakened the vegetation carbon sequestration services and biodiversity services in the plateau ecosystem. Therefore, first of all, the monitoring system of ultra meteorological calamity should be built to improve the risk-resistance ability and recovery capability of forestry and agriculture to cope with extreme meteorological calamity, and reduce the economic losses caused by forestry disasters (Shen et al., 2023). Secondly, the vegetation species structure and ecological connectivity should be improved through ecological management. Third, promote scientific farming methods, prevent the degradation of plateau ecosystems and arid regions, and improve the carbon sequestration capacity of vegetation and soil as well as water and soil conservation capacity. (2) Optimize the industrial structure and establish a green and sustainable industrial system. In the URYR, since the enforcement of western grand development tactic and the enforcement of the policy of the midwestern regions to undertake the industrial transfer from the east, the development of resource-based industries and investment in real estate have become the dominating growth points and driving forces of regional economy. Nonetheless, the development level of high-end manufacturing and high-tech industries is relatively low. The industrial structure in the URYR shows a "23" type, the economic growth mainly relies on the secondary industry, and the tertiary industry is relatively backward compared with the country. Therefore, we should promote the decoupling of industrial development and carbon emission reduction, increase investment in high-tech industries and modern service industries, establish a green and sustainable industrial system, and adopt a low-carbon path of low energy consumption and high development. (3) Promote moderate, intensive and green

urbanization. Previous studies have proposed (Feng et al., 2021) that urbanization rate has a positive direct impact and cumulative effect on carbon emissions, and that a 1% increase in urbanization rate will lead to an increase of about 1.61% in carbon emissions. The provinces in the URYR are experiencing rapid urbanization growth and thus contribute significantly to the aggrandize in carbon emissions. Therefore, we should be restricted urban expansion and improve the urban land intensive use level. On the other hand, the developmental ideal of green and low-carbon should be integrated into the urbanization development planning, and a protective and cooperative land use pattern should be built through the planning and control of main functional zones.

Innovation points and shortcomings

The dominating innovations of this study: Firstly, this study proposes a more comprehensive multi-scenario simulation framework for the carbon budget. Secondly, the influencing factors of provincial carbon emissions were analyzed. Thirdly, the time evolution of carbon balance from 2030 to 2100 under different SSP scenarios was simulated, and the optimal low-carbon development path for each province is proposed. Fourth, from the perspective of comprehensive regulation and control, the carbon balance regulation and control strategy is proposed to provide decision-making basis for urban low-carbon development and regional carbon neutrality.

This study has improved the relevant research on multi-scenario prediction of carbon balance to a certain extent, but there are still the following shortcomings: (1) In terms of research scale, due to the limited availability of data and the large workload, this study is based on regional scale and provincial scale, but it will lead to the loss of spatial details. In future studies, it can be refined from the provincial scale to the municipal scale, to identify cities with high net carbon emissions in this region, and further provide corresponding suggestions for different types of cities to reduce carbon emissions and increase carbon absorption. (2) In terms of carbon emission accounting, the emission coefficient of different regions and industries in the YRB will change with the development of socioeconomic and the advance of technology. Therefore, there is some uncertainty in the carbon emission coefficient. In future research, it is hoped to establish a real-time monitoring and release mechanism of carbon emission coefficient between different departments or industries, so as to further improve the accuracy and efficiency of the research.

Conclusion

Based on the perspective of carbon balance, this study carried out a long time series, multi-scenario carbon budget forecast for the YRB, and put forward the regulation strategies of carbon balance for different regions. The main conclusions are as follows:

(1) Carbon sequestration stock and carbon emissions in the YRB show a trend of fluctuating increase during 2000-2020, but the growth rate of carbon emissions is far greater than carbon storage stock. The net carbon emission in the YRB during 2000-2020 is negative, which is represented as a carbon sink area. From the perspective of net carbon emissions by provinces, the net carbon emissions of Inner Mongolia, Qinghai, Shaanxi and Gansu were negative during 2000-2020, while the net carbon emissions of Shandong were positive. Henan, Shanxi and Ningxia were transformed from carbon sink regions to carbon source regions in 2003, 2006 and 2007, respectively.

(2) Under the SSP1-5 scenario, the order of carbon sequestration of all provinces in the YRB during 2030-2100 is consistent, namely Inner Mongolia, Qinghai, Shaanxi, Gansu, Shanxi, Henan, Ningxia and Shandong. In terms of time evolution, the carbon storage in Qinghai, Shaanxi, Gansu, Shanxi, Inner Mongolia, Ningxia and Shandong all showed a slow rise, but the growth rate of SSP1, SSP2 and SSP4 scenarios was higher than that of SSP3 and SSP5 scenarios.

(3) The STIRPAT model can be used to predict the carbon emissions of the YRB in the future with high precision. Under the SSP1-5 scenario, the carbon emissions in Inner Mongolia, Qinghai and Shandong show a downward trend during 2030-2100, while the overall carbon emissions in Gansu, Henan, Shaanxi, Shanxi and Ningxia show an upward trend. Compared with different scenarios, the carbon emissions in Gansu, Henan, Shaanxi, Shanxi and Ningxia reached the lowest level under SSP2 and SSP3 scenarios.

(4) In terms of net carbon emissions, under the SSP1-5 scenario, the YRB will be a carbon sink area from 2030 to 2080, and a carbon source area from 2080 to 2100. The sharp increase of carbon emissions and the slow rise of carbon sequestration stock lead to the extreme imbalance of the carbon system in the YRB. Therefore, effective measures should be taken to enhance the terrestrial carbon absorption capacity and reduce the pressure of carbon emissions.

(5) Different provinces have different paths to low-carbon development, Inner Mongolia and Qinghai maintain a good low-carbon development path under SSP1, SSP2 and SSP4 scenarios, Ningxia and Shandong maintain a good low-carbon development path under SSP1 and SSP2 scenarios, Shanxi maintains a good low-carbon development path under SSP1 and SSP3 scenarios, Gansu, and Shaanxi and Henan maintain a good low-carbon development path under the SSP3 scenario.

Acknowledgements. This research was supported by the National Natural Science Foundation of China (42101206), Henan Science and Technology Innovation Talent Project (24HASTIT050), Outstanding Youth Science Fund of Henan Province (242300421144), Henan Graduate Excellent Teaching Case Project (YJS2024AL122), the Key Research Project of Higher Education Institutions of Henan Province (24A170023, 24B170008). The authors thank the reviewers of this paper for their insights and comments.

REFERENCES

- [1] Bontemps, S., Herold, M., Kooistra, L., van Groenestijn, A., Hartley, A., Arino, O., Moreau, I., Defourny, P. (2012): Revisiting land cover observation to address the needs of the climate modeling community. – *Biogeosciences* 9(6): 2145-2157.
- [2] Chen, Y., Guo, F., Wang, J., Cai, W., Wang, C., Wang, K. (2020): Provincial and gridded population projection of China under shared socioeconomic pathways from 2010 to 2100. – *Scientific Data* 7: 83.
- [3] Fang, K., Tang, Y. Q., Zhang, Q. F. (2019): Will China peak its energy-related carbon emissions by 2030? Lessons from 30 Chinese provinces. – *Applied Energy* 255: 113852.
- [4] Feng, D. L., Liu, M., Liu, S. (2021): Analysis of the Current Status and Development Strategy of Low-Carbon Economy in the Upper Yellow River Economic Belt. – *Ecological Economic* 37(3): 13-22.
- [5] Han, M. Y., Liu, W. D., Yang, M. Y. (2022): Carbon risk transmission of China's energy-intensive industries under low-carbon transition: From the embodied carbon network perspective. – *Geography Research* 41(1): 79-91.

- [6] He, J., Li, Z., Zhang, X., Wang, H., Dong, W. (2022): Towards carbon neutrality: a study on China's long-term low-carbon transition pathways and strategies. – *Environmental Science and Ecotechnology* 9(1): 100134.
- [7] Huang, R., Wang, Z., Ding, G. Q. (2016): Trend prediction and analysis of influencing factors of carbon emissions from energy consumption in Jiangsu province based on STIRPAT model. – *Geography Research* 35(4): 781-789.
- [8] Ji, K., Peta, A. (2021): The development of carbon capture utilization and storage (CCUS) research in China: A bibliometric perspective. – *Renewable and Sustainable Energy Reviews* 138: 110521.
- [9] Jiang, W. B., Liu, W. D. (2021): Effect of change of the spatial pattern of economic activities on CO₂ emissions in China. – *Resource Science* 43(4): 722-732.
- [10] Jiao, W. X., Chen, X. P. (2012): Environmental impact analysis of Gansu Province based on STIRPAT model. – *Resources and Environment in the Yangtze Basin* 21(1): 105-110.
- [11] Li, W. J., Xie, S. Y., Wang, Y., Huang, J., Cheng, X. (2021): Effects of urban expansion on ecosystem health in Southwest China from a multi-perspective analysis. – *Journal of Cleaner Production* 294: 126341.
- [12] Liu, Z., Guan, D. B., Moore, S. (2015): Climate policy: Steps to China's carbon peak. – *Nature* 522(7556): 279-281.
- [13] Liu, G. X., Wang, X. J., Xiang, A. C., Wang, X. R. (2021): Spatial heterogeneity and driving factors of land use change in the middle and upper reaches of Ganjiang River, southern China. – *Chinese of Applied Ecology* 32(7): 2545-2554.
- [14] Liu, P., Liu, L., Xu, X., Zhao, Y. (2021): Carbon footprint and carbon emission intensity of grassland wind farms in Inner Mongolia. – *Journal of Cleaner Production* 313: 127878.
- [15] Liu, J., Pei, X., Zhu, W., Jiao, J. (2023): Multi-scenario simulation of carbon budget balance in arid and semi-arid regions. – *Journal of Environmental Management* 346: 119016.
- [16] Luo, M., Hu, G., Chen, G. (2022): 1 km land use/land cover change of China under comprehensive socioeconomic and climate scenarios for 2020–2100. – *Scientific Data* 9: 110.
- [17] Ma, X., Jiang, P., Jiang, Q. (2020): Research and application of association rule algorithm and an optimized grey model in carbon emissions forecasting. – *Technological Forecasting and Social Change* 158: 120159.
- [18] Mo, H. B., Wang, S. J. (2021): Spatio-temporal evolution and spatial effect mechanism of carbon emission at county level in the Yellow River Basin. – *Scientia Geographica Sinica* 41(8): 1324-1335.
- [19] Mudryk, L. R., Dawson, J., Howell, S. E. L., Derksen, C. (2021): Impact of 1, 2 and 4° C of global warming on ship navigation in the Canadian Arctic. – *Nature Climate Change* 11: 673-679.
- [20] Pan, W. B., Fu, H. M., Zheng, P. (2020): Regional Poverty and Inequality in the Xiamen-Zhangzhou-Quanzhou City Cluster in China Based on NPP/VIIRS Night-Time Light Imagery. – *Sustainability* 12(6): 2547.
- [21] Peng, W., Xin, B. G., Xie, L. (2023): Optimal strategies for production plan and carbon emission reduction in a hydrogen supply chain under cap-and-trade policy. – *Renewable Energy* 215: 118960.
- [22] Regnier, P., Resplandy, L., Najjar, R. G., Ciais, P. (2023): The land-to-ocean loops of the global carbon cycle. – *Nature*, 603(16): 401-410.
- [23] Shen, W., Li, Y., Qin, Y. C. (2023): Research on the influencing factors and multi-scale regulatory pathway of ecosystem health: A case study in the Middle Reaches of the Yellow River, China. – *Journal of Cleaner Production* 406: 137038.
- [24] Shen, W., Li, Y., Qin, Y. C. (2023): Influencing mechanism of climate and human activities on ecosystem health in the Middle Reaches of the Yellow River of China. – *Ecological Indicators* 150: 110191.

- [25] Tang, L. P., Ke, X. L., Zhou, Q. S. (2020): Projecting future impacts of cropland reclamation policies on carbon storage. – *Ecological Indicators* 119: 106835.
- [26] VanHoek, W., Wang, J. J., Vilmin, L. (2021): Exploring Spatially Explicit Changes in Carbon Budgets of Global River Basins during the 20th Century. – *Environmental Science and Technology* 55(24): 16757-16769.
- [27] Wang, S. J., Huang, Y. Y., Zhou, Y. Q. (2019): Spatial spillover effect and driving forces of carbon emission intensity at the city level in China. – *Journal of Geographical Sciences* 74(6): 1131-1148.
- [28] Wang, X. G., Li, G. (2020): Effect of "Ecological Province" construction on carbon emission reduction in China. – *Acta Geographica Sinica* 75(11): 2431-2442.
- [29] Wang, S. J., Gao, S., Huang, Y. Y. (2020): Spatio-temporal evolution and trend prediction of urban carbon emission performance in China based on super-efficiency SBM model. – *Acta Geographica Sinica* 75(6): 1316-1330.
- [30] Wang, C., Zhan, J. Y., Zhang, F., Liu, W. (2021): Analysis of urban carbon balance based on land use dynamics in the Beijing-Tianjin-Hebei region, China. – *Journal of Cleaner Production* 281: 125138.
- [31] Wang, X., Che, L., Zhou, L., Xu, J. G. (2021): Spatio-temporal Dynamic Simulation of Land use and Ecological Risk in the Yangtze River Delta Urban Agglomeration, China. – *Chinese Geographical Science* 31(5): 829-847.
- [32] Wang, T. T., Sun, F. B. (2022): Global gridded GDP data set consistent with the shared socioeconomic pathways. – *Scientific Data* 9: 221.
- [33] Wang, Y. L., Liang, D. D., Wang, J. (2023): An analysis of regional carbon stock response under land use structure change and multi-scenario prediction, a case study of Hefei, China. – *Ecological Indicators* 151: 110293.
- [34] Wu, N. L., Yang, S. T., Liu, X. Y., Luo, Y. (2014): Response analysis of land use change to the degree of human activities in Beiluo River basin since 1976. – *Acta Geographica Sinica* 69(1): 54-63.
- [35] Xia, C. Y., Li, Y., Xu, T. B. (2019): Analyzing spatial patterns of urban carbon metabolism and its response to change of urban size: A case of the Yangtze River Delta, China. – *Ecological Indicators* 104: 615-625.
- [36] Xu, C. L., Zhang, Q. B., Yu, Q., Wang, J. P. (2023): Effects of land use/cover change on carbon storage between 2000 and 2040 in the Yellow River Basin, China. – *Ecological Indicators* 151: 110345.
- [37] Xue, H., Shi, Z., Huo, J., Zhu, W., Wang, Z. (2023): Spatial difference of carbon budget and carbon balance zoning based on land use change: a case study of Henan Province, China. – *Environmental Science and Pollution Research* 30(9): 109145-109161.
- [38] Zhang, H., Peng, Q. R., Wang, R., Qiang, W. L., Zhang, J. X. (2020): Spatiotemporal patterns and factors influencing county carbon sinks in China. – *Acta Ecologica Sinica* 40(24): 8988-8998.
- [39] Zhang, Y., Shi, X. Y., Tang, Q. (2021): Carbon storage assessment in the upper reaches of the Fenhe River under different land use scenarios. – *Acta Ecologica Sinica* 41(1): 360-373.
- [40] Zhang, K., Zhu, C., Ma, X., Zhang, X., Yang, D. (2023): Spatiotemporal Variation Characteristics and Dynamic Persistence Analysis of Carbon Sources/Sinks in the Yellow River Basin. – *Remote Sensing* 15(2): 323.
- [41] Zheng, H. L., Zheng, H. F. (2023): Assessment and prediction of carbon storage based on land use/land cover dynamics in the coastal area of Shandong Province. – *Ecological Indicators* 154: 110474.
- [42] Zhou, S., Tong, Q., Pan, X. Z. (2021): Research on low-carbon energy transformation of China necessary to achieve the Paris agreement goals: A global perspective. – *Energy Economic* 95: 105137.